Microstructure of Poly[(*R*,*S*)-β-hydroxybutyrate] by ^{13}C NMR

Philippa J. Hocking and Robert H. Marchessault*

Department of Chemistry, McGill University, 3420 University Street, Montreal, Quebec, Canada H2A 3A7

Received March 20, 1995; Revised Manuscript Received June 15, 1995[⊗]

ABSTRACT: High-resolution ^{13}C NMR spectra were obtained for a wide tacticity range of racemic poly[(*R*,*S*)-β-hydroxybutyrate] samples and interpreted with regard to several statistical models. None of the samples followed Bernoullian statistics, but the syndiotactic and atactic fractions essentially obeyed first-order Markov statistics, as derived for racemic monomer. Fitting to a second-order Markovian model confirmed previously-held theories regarding the blocky nature of the polymer. An enantiomorphic model described the more isotactic samples well but did not adequately describe the atactic and syndiotactic ones; a two-site model involving enantiomorphic and first-order Markovian sites was therefore proposed, and the parameters necessary to describe each sample were calculated. Average isotactic and syndiotactic block lengths were also calculated and used in the interpretation of degradation and single-crystal results.

Introduction

Poly(β-hydroxybutyrate) (PHB) is a natural polyester whose current notoriety is due to its inherent biodegradability.[1−6] The method of choice for large-scale production is bacterial fermentation; this yields perfectly isotactic polymer, where the chiral center in each repeat unit is solely *R* in absolute configuration. An alternative biosynthetic route is currently under development,[7,8] where the polyester is produced in genetically altered plants. Synthetic approaches to optically active PHB include the polymerization of optically active monomer[9] and use of stereoselective catalysts with racemic monomer.[10,11] Synthetic methods can also yield material not available by biosynthetic methods, such as the racemic polyester, poly[(*R*,*S*)-β-hydroxybutyrate], which is useful for studies on the effects of stereochemistry on structure, properties, and enzymatic degradability and has potential as a blend component.

A significant discovery in the development of (*R*,*S*)-PHB was that racemic β-butyrolactone can be ring-opened to yield crystalline polymer, the crystalline structure of which is identical by X-ray diffraction to that of fully isotactic polymer isolated from bacteria.[12] Such results have been reported using a variety of aluminoxane catalysts;[9,13−17] the attainment of an isotactic crystal structure from racemic monomer polymerized with a nonstereospecific catalyst is attributed to the existence of a stereoblock structure involving either blocks of both enantiomers in the same chain or separate chains of each.[12,14,16,18,19] Quantitation of the level of stereoregularity achieved has been possible by ^{13}C and ^{1}H NMR, where peak expansions reveal fine structure due to variation in stereosequence. Although this stereosensitivity appears for all peaks, resolution is usually best for the isotactic and syndiotactic diad components of the carbonyl peak in ^{13}C NMR, making this the signal of choice for quantitation. Without quantitative information about longer stereosequences, questions about the statistics of the polymerization mechanism and the exact nature of the stereoblock structure have remained unanswered.

Recently, a predominantly syndiotactic form of crystalline (*R*,*S*)-PHB has been reported.[20−25] The largest yields of this material have been obtained using tin-based catalysts,[21−25] which specifically select for the syndiotactic structure, but small amounts of syndiotactic material have also been isolated from the same aluminoxane catalysts as were developed for the isotactic polymer.[20] Simultaneous improvements in NMR technology have improved the resolution attainable in the ^{13}C NMR spectrum, such that triad sensitivity in the methylene region of the spectrum can now be observed[21,25] and quantified.[23,24] This allows more detailed analysis of the microstructure of the synthetic polymer than was previously possible, which should prove particularly interesting for the aluminoxane-catalyzed polymer, given the wide tacticity range spanned by a single reaction.

Previous statistical analysis of polymers within the PHB family by NMR intensities includes investigation of the sequence of butyrate and valerate in poly(β-hydroxybutyrate-*co*-β-hydroxyvalerate) isolated from bacteria,[26−29] where all asymmetric carbons have an absolute *R* configuration so variation in stereosequence cannot occur; as the chemical shift differences between butyrate and valerate are greater than those between isotactic and syndiotactic PHB, resolution of the varying sequences was more attainable. Stereosequences were observed in synthetic poly[(*R*,*S*)-β-hydroxybutyrate-*co*-(*R*,*S*)-β-hydroxyvalerate],[19,30] but statistical interpretations could not be applied as only diad stereosequences were resolved. Until recently, a similar situation existed for (*R*,*S*)-PHB; preliminary statistical interpretation of diad and triad intensities for (*R*,*S*)-PHB involved mainly syndiotactic PHB.[23] In another study,[24] diad and triad intensities were measured over a wide tacticity range, but statistical interpretation was not attempted due to the complications of varying *R*/*S* monomer ratios.

Determination of the microstructure of (*R*,*S*)-PHB takes on a practical as well as theoretical importance in aiding in the interpretation of enzymatic degradation results. As there is clearly a correlation between tacticity and enzymatic degradation rate,[24,31−35] the question arises as to the minimum isotactic block length which can still be cleaved by PHB depolymerases. Calculation of the average isotactic block lengths in a wide tacticity range of samples, the degradability of which has already been tested,[34,35] can therefore provide an indication as to the dependence of degradation behavior on block length. Average block lengths could also relate to the formation of single crystals from some of these (*R*,*S*)-PHB samples;[36,37] the ease with which

[⊗] Abstract published in *Advance ACS Abstracts,* August 1, 1995.

0024-9297/95/2228-6401$09.00/0

Table 1. Diad and Triad Designations Relevant for (*R*,*S*)-PHB

	stereosequence	designation	configuration
diads	isotactic	*i*	*RR* + *SS*
	syndiotactic	*s*	*RS* + *SR*
triads	isotactic	*ii*	*RRR* + *SSS*
	syndiotactic	*ss*	*RSR* + *SRS*
	heterotactic-1	*is*	*RRS* + *SSR*
	heterotactic-2	*si*	*RSS* + *SRR*

such crystals can be formed from the more isotactic fractions suggests that the average isotactic block length could be comparable to the average lamellar thickness.

In this study, various fractions of (*R*,*S*)-PHB covering a wide tacticity range were examined by high-resolution solution NMR and examined with regard to the following statistics. As the statistics for determining the microstructure of vinyl polymers[38-41] are not directly applicable to PHB, the necessary modifications[42] to the theory are discussed first. Average isotactic and syndiotactic block lengths were also calculated. Proton-decoupled ^{13}C NMR was used in preference to ^{1}H NMR due to the wider chemical shift range (~0−200 ppm, instead of ~0−10 ppm) and the absence of spin−spin coupling.

Theory

Differences between PHB and Vinyl Chains. Because the symmetry of the connecting group between asymmetric carbons is not the same as that in a vinyl polymer, PHB diads are not "meso" or "racemic"; they are, however, "isotactic" and "syndiotactic" and so can be accurately represented by "*i*" and "*s*". The absolute stereochemistry of each repeating unit in (*R*,*S*)-PHB means that there are two possible configurations for each stereosequence, as shown in Table 1. Although, in the absence of a chiral resolving agent, the two configurations for each stereosequence are indistinguishable from each other by NMR, the *is* and *si* heterotactic triads are distinct structures which should appear at different chemical shifts (Figure 1). Such differences necessitate modifications in the statistics used to describe the polymer.

Bernoullian Model. Under Bernoullian statistics, successive additions of *R* and *S* monomer are independent events, so the rates of addition of *R* and *S* monomer to the growing chain end are not affected by the configuration of the last repeating unit. The probability of any given stereosequence can then be described by a single parameter, P_R, where P_R is the mole fraction of *R* repeat units in the polymer, which should also equal the proportion of *R* repeat units in the starting monomer. P_S is then $1 - P_R$. Relations between sequences of different orders in these Bernoullian statistics have been described and plotted[42] as a function of P_R; in the case where the starting monomer is racemic, $P_R = P_S = 0.50$, and the triad intensities are $ii = ss = is = si = 0.25$.

First-Order Markov Model. For first-order Markov statistics, the addition of the new monomer to the growing chain is influenced by the configuration of the last repeating unit of the chain. Thus, as for vinyl polymers, first-order Markov statistics involves two independent parameters, now $P_{R/S}$ and $P_{S/R}$, and two dependent variables, $P_{R/R} = 1 - P_{S/R}$ and $P_{S/S} = 1 - P_{R/S}$, where $P_{R/S}$ is the probability of adding *R* monomer to an *S* chain end. Stereosequence relations involving these parameters have been derived[42] in the general case, valid for every possible P_R; care must be taken to account for continuous variation in the composition and hence tacticity of the polymer as the composition of the unreacted monomer changes.

The only case in which the composition of unreacted monomer remains constant is when the starting monomer is racemic, so $P_R = P_S = 0.5$. In this case, $P_{R/R} = P_{S/S}$ and $P_{R/S} = P_{S/R}$, which simplifies the relations between the conditional probabilities and the stereosequences such that diad and triad intensities can be calculated using the single conditional probability, $P_{R/R}$:

$$i = P_{R/R} \qquad s = 1 - P_{R/R} \qquad ii = P_{R/R}^2$$
$$is = si = P_{R/R}(1 - P_{R/R}) \qquad ss = (1 - P_{R/R})^2 \quad (1)$$

Given the similarity between these relations and Bernoullian relations for vinyl chains, a modified Bernoullian test parameter[39] can be defined to test for the first-order Markov mechanism in PHB, by

$$B_2 = 4(ii)(ss)/(is + si)^2 \quad (2)$$

where a value close to 1.0 indicates adherence to the mechanism. Thus, although tetrad intensities are required to test for first-order Markov statistics in a vinyl polymer, the mechanism can be tested in racemic PHB based on only triad intensities.

Second-Order Markov Model. For second-order Markov statistics, where the addition of new monomer is affected by the configuration of the last two units of the existing chain, four independent parameters are required: $P_{R/SS}$, $P_{R/SR}$, $P_{S/RR}$, and $P_{S/RS}$, where $P_{S/RS}$ is the probability of adding an *S* repeating unit to an existing *RS* diad. In the case of racemic monomer, $P_{R/SS} = P_{S/RR}$ and $P_{R/SR} = P_{S/RS}$, so the polymer can be described[42] using only $P_{R/SS}$ and $P_{R/SR}$, calculated as follows:

$$P_{R/SS} = \frac{(is + si)}{2(ii) + (is + si)} \qquad P_{R/SR} = \frac{(is + si)}{2(ss) + (is + si)} \quad (3)$$

As these expressions are remarkably similar to those for first-order Markov statistics in vinyl polymers,[38-40] other interpretations from vinyl statistics can also be applied. Thus, $P_{R/SS} + P_{R/SR} = 1$ indicates adherence to a racemic first-order Markov mechanism, and the values of the conditional probabilities can be interpreted[39,40] as:

block: $P_{R/SS} < 0.5$, $P_{R/SR} < 0.5$

$$P_{R/SS} + P_{R/SR} < 1$$

heterotactic-like (alternating):

$$P_{R/SS} > 0.5, \quad P_{R/SR} > 0.5$$

$$P_{R/SS} + P_{R/SR} > 1 \quad (4)$$

isotactic-like: $P_{R/SS} < 0.5$, $P_{R/SR} > 0.5$

syndiotactic-like: $P_{R/SS} > 0.5$, $P_{R/SR} < 0.5$

If a modified persistence ratio[39,40,43,44] is defined using

$$\varrho_2 = 2(i)(s)/(is + si) \quad (5)$$

the extent to which ϱ_2 is greater than 1.0 indicates the tendency to blockiness, and $\varrho_2 = (P_{R/SS} + P_{R/SR})^{-1}$ for

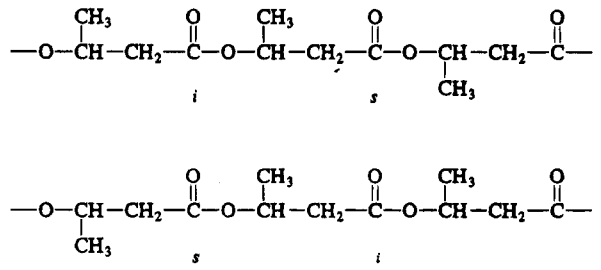

Figure 1. Heterotactic triads of (*R,S*)-PHB.

racemic polymer obeying second-order Markov statistics. As for the first-order Markov mechanism in vinyl polymers, the second-order Markov probabilities can be calculated from triad intensities, but the model cannot actually be tested without longer stereosequences.

Enantiomorphic Model. An alternative model for isotactic polymerization is that of enantiomorphic catalyst sites,[45,46] where the catalyst is considered to consist, at any given time, of an equal number of *R*- and *S*-preferring sites. Therefore, the configuration of the adding monomer is primarily determined by the catalyst itself, rather than by the existing polymer chain end. The probability of an *R* unit following an *R* unit, P_{RR}, at an *R*-preferring site, thus equals the probability of an *R* unit following an *S* unit, P_{SR}, at the same site, while the probability of an *S* unit following an *S* unit, P_{SS}, or of an *S* unit following an *R* unit, P_{RS}, at the same *R*-preferring site, is substantially lower. Triad intensities can be calculated[46] by

$$(ii) = 1 - 3(\alpha - \alpha^2) \tag{6}$$

$$(ss) = \alpha - \alpha^2 \tag{7}$$

$$(is + si) = 2(\alpha - \alpha^2) \tag{8}$$

where α is the value of P_{RR} at an *R*-preferring site or of P_{SS} at an *S*-preferring site. The extent to which such a model accurately describes a given polymer chain can be determined[47] by calculating the test parameters

$$E_1 = 2(ss)/(is + si) \tag{9}$$

and

$$E_2 = 1 - \frac{4}{(is + si) + 2(ss)} + \frac{1}{(ss)} \tag{10}$$

where, for a polymer following the model, $E_1 = E_2 = 1$.

Two-Site Model. For racemic monomer, the enantiomorphic and first-order Markovian models can be combined to give a two-site model, in a manner similar to that used for enantiomorphic and Bernoullian models for polypropylene.[47-51] According to this model, the polymer is created at both sites simultaneously, yielding either chains of different configurations or, through a dynamic equilibrium of chain ends,[43,52] stereoblocks of different configurations in the same chain. Triad equations, adjusted for racemic monomer, use σ_2 for $P_{R/R}$ at the first-order Markov sites, α for P_{RR} at the *R*-preferring enantiomorphic sites, and a weighting factor ω to describe the proportion of the polymer formed at the enantiomorphic site, as follows:

$$(ii) = \omega[1 - 3(\alpha - \alpha^2)] + (1 - \omega)\sigma_2^2 \tag{11}$$

$$(is + si) = \omega[2(\alpha - \alpha^2)] + (1 - \omega)[2\sigma_2(1 - \sigma_2)] \tag{12}$$

$$(ss) = \omega(\alpha - \alpha^2) + (1 - \omega)[(1 - \sigma_2)^2] \tag{13}$$

For fractionated polymer from the same polymerization reaction, α and σ_2 should be relatively constant, with the value of ω varying to reflect the varying contribution by each site to each of the fractions.

Average Block Lengths. The average lengths of isotactic and syndiotactic blocks, $\bar{n}_i$ and $\bar{n}_s$, respectively, can be calculated from diad and triad intensities; since $\bar{n}_i$ and $\bar{n}_s$ are defined in terms of diads, the actual number of monomer units involved in such sequences are $\bar{n}_i + 1$ and $\bar{n}_s + 1$. These values can be calculated[39,41] independently of the polymerization mechanism using

$$\bar{n}_i = \frac{1 - (ii)/(ss)}{1 - ((s)/(i))((ii)/(ss))} \quad \text{and} \quad \bar{n}_s = \frac{1 - (ii)/(ss)}{(i)/(s) - (ii)/(ss)} \tag{14}$$

More specific block length equations can be derived for defined polymerization mechanisms.[38-40,53]

Experimental Section

Description of Samples. Polymer samples were obtained by bulk ring-opening polymerization of racemic β-butyrolactone with a preformed methylaluminoxane or *in situ* triisobutylaluminum/water [Al(iBu)$_3$/H$_2$O, 1:1 (mol/mol)] catalyst, using vacuum techniques. The isolated polymer was fractionated by solubility in chloroform/methanol and in acetone, yielding fractions ranging from primarily syndiotactic to highly isotactic. Original characterization in terms of percent isotactic diads, used to provide the samples with working names, was obtained by ^{13}C NMR using 0.03 g/mL polymer solutions in $CDCl_3$ on a JEOL CPF-270 spectrometer at 67.8 MHz, with a spectral window of 18 050 Hz, an acquisition time of 0.908 s, a pulse width of 30°, and a pulse delay of 0.8 s. The identification of samples by low-resolution percent isotactic diads provides an immediate indication as to whether each is isotactic (more than 50% isotactic diads), atactic (near 50% isotactic diads), or syndiotactic (less than 50% isotactic diads). Details of the polymerization, fractionation, and characterization have been previously published.[20]

High-Resolution ^{13}C NMR. High-resolution ^{13}C NMR spectra were obtained for 0.03–0.05 g/mL solutions in a variety of solvents at various temperatures on a Unity-500 spectrometer at 125 MHz. Spectra in $CDCl_3$ were accumulated at room temperature, with a spectral window of 30 007.5 Hz, a pulse width of 90°, an acquisition time of 2.133 s, a pulse delay of 8 s, 1500–4000 transients, and 128 000 data points, for a spectral resolution of 0.234 Hz/point; processing included zerofilling (fn = 262 144) and resolution enhancement (line broadening (lb) = −1.46, Gaussian factor (gf) = 0.392). Spectra in tetrachloroethane-d_2 (TCE) were accumulated (700–2000 transients) at 110 °C, under the same conditions but with the delay time increased to 20 s to allow for the increase in T_1 with temperature. Processing again included zerofilling, but less resolution enhancement was required (typically, lb = −0.80, gf = 0.572). To reduce the probability of thermal degradation, all tubes were purged with dry nitrogen immediately prior to analysis; comparison of ^{1}H NMR spectra run immediately after equilibration at 110 °C and after acquiring the ^{13}C NMR spectra showed that no NMR-observable changes occurred during acquisition of the ^{13}C spectra. Peak intensities were measured by spectrometer integration; in the cases where peaks overlapped, peak-fitting routines gave similar results.

Results and Discussion

Solvent Testing. Various solvents and temperatures were tested for resolution improvement over the

Table 2. Variation in Resolution of Carbonyl Diads and Methylene Triads of (*R,S*)-PHB as a Function of Solvent and Temperature

solvent	bp (°C)	spectrom temp (°C)	resolution (microstructure visible)
acetone-d_6	57	45	partly split diads, triads
benzene-d_6	80	65	diads, triads
$CDCl_3$	61	50	partly split diads, triads
$CDCl_3$	61	RT	partly split diads, triads
DMF-d_7	153	110	diads, partial triads
DMSO-d_7	189	110	diads only, triads overlap with solvent
pyridine-d_5	116	100	diads, triads
TCE-d_2	147	110	diads, triads
toluene-d_8	111	100	diads, triads

traditional $CDCl_3$ at room temperature. The (*R,S*)-PHB sample with 45% isotactic diads was used for this study, as a relatively soluble fraction where all the diad and triad components have significant intensity. Spectra were obtained at temperatures as high[54-56] as the solvent boiling points would permit and processed without resolution enhancement; the carbonyl (~169 ppm) and methylene (~41 ppm) regions were then expanded to observe the extent to which diad and triad fine structure were resolved (Table 2). None of the solvents tested gave significantly better resolution than $CDCl_3$, and several gave significantly worse resolution, had solvent peaks interfering with the sample peaks of interest, or would be unlikely to dissolve the more isotactic (less soluble) fractions. Accordingly, the solvent/temperature conditions selected were $CDCl_3$ at ambient temperature and TCE-d_2 at 110 °C; comparison of the results from these two different systems should indicate the extent to which the results obtained are specific to the solvent/temperature choice.

Spectral Assignments. Expansion of any of the four peaks in the ^{13}C NMR spectrum of (*R,S*)-PHB reveals fine structure resulting from the various stereosequences.[21] Because the resolution of this fine structure is better in the carbonyl (~169 ppm) and methylene (~41 ppm) regions of the spectrum than in the methyl (~20 ppm) and methine (~67.5 ppm) regions, the analysis which follows focuses on the former two regions. As the distance between asymmetric centers in PHB is twice as large as that in vinyl polymers, resolution over the same number of bonds in PHB involves only half as many repeat units.

The resolution of the methylene region of (*R,S*)-PHB was similar to that previously reported,[21,23-25] and the variations in triad intensity with changes in the low-resolution diad content (Figure 2) were consistent with these earlier assignments. The assignments of *is* and *si* are based on the assumptions that the *is* triad derives from the *s* diad, and the *si* triad, from the *i* diad, as previously discussed;[21] this assignment implies that the chain is drawn as in Figure 3, which agrees with the IUPAC guidelines for selection and orientation of the constitutional repeating unit.[57] Because the *si* and *is* terms are summed when used in the equations, reversing these assignments would not change the results of the calculations.

In the carbonyl region, particularly in the $CDCl_3$ spectra, four components are clearly visible (Figure 4), instead of the expected two. Previously observed splitting of the higher field racemic component[21] has been attributed to partial resolution of the *RS* and *SR* sequences, despite the low probability of distinguishing this difference in the absence of a chiral resolving agent. This logic implies that the splitting of the meso component results from partial resolution of the *RR* and *SS* sequences, which causes difficulty in explaining why one of these components decreases sharply in intensity with increasing isotacticity. A more likely explanation for the extra splitting is that it results from partly resolved tetrads, with the lower field pair comprising the *s*-centered tetrads and the higher field pair comprising the *i*-centered tetrads. The variations in component intensities imply that the downfield component of the syndiotactic diad peak represents the *ssi* and *iss* tetrads, with the *sss* and *isi* tetrads further upfield; similarly, for the isotactic diads, the downfield component includes the *iii*, *sii*, and *iis* tetrads, with the *sis* tetrad slightly upfield. As only one tetrad is individually resolved, it is not possible to apply calculations requiring individual tetrad intensities to these data; therefore, in the calculations which follow, only diad and triad intensities were

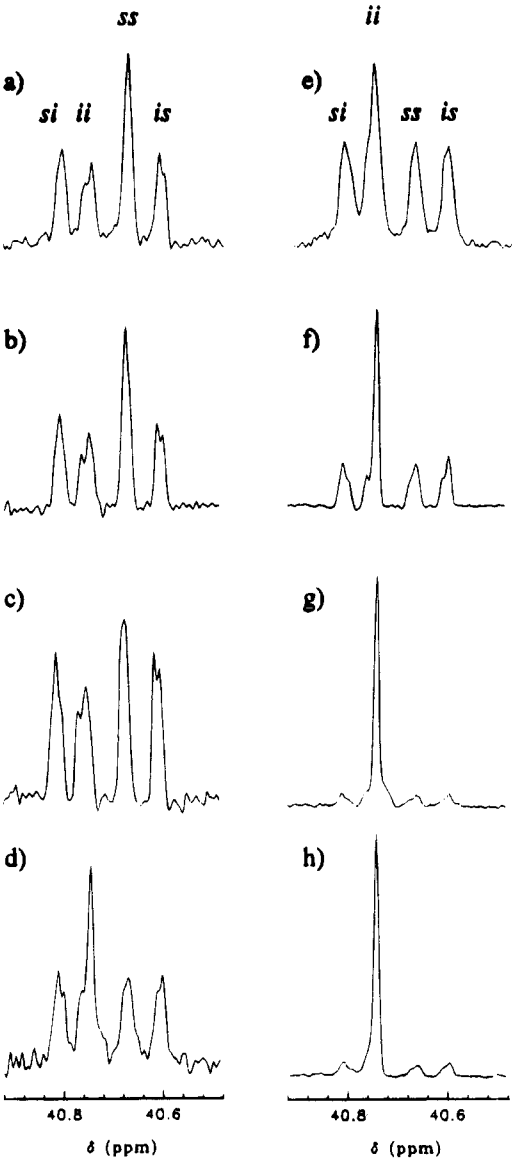

Figure 2. Expansions of the methylene resonances for (*R,S*)-PHB in $CDCl_3$ at room temperature: (a) sample with 34% isotactic diads; (b) 40% isotactic diads; (c) 45% isotactic diads; (d) 55% isotactic diads; (e) 60% isotactic diads; (f) 68% isotactic diads; (g) 79% isotactic diads; and (h) 88% isotactic diads.

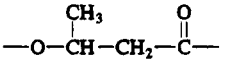

Figure 3. Constitutional repeating unit of PHB.

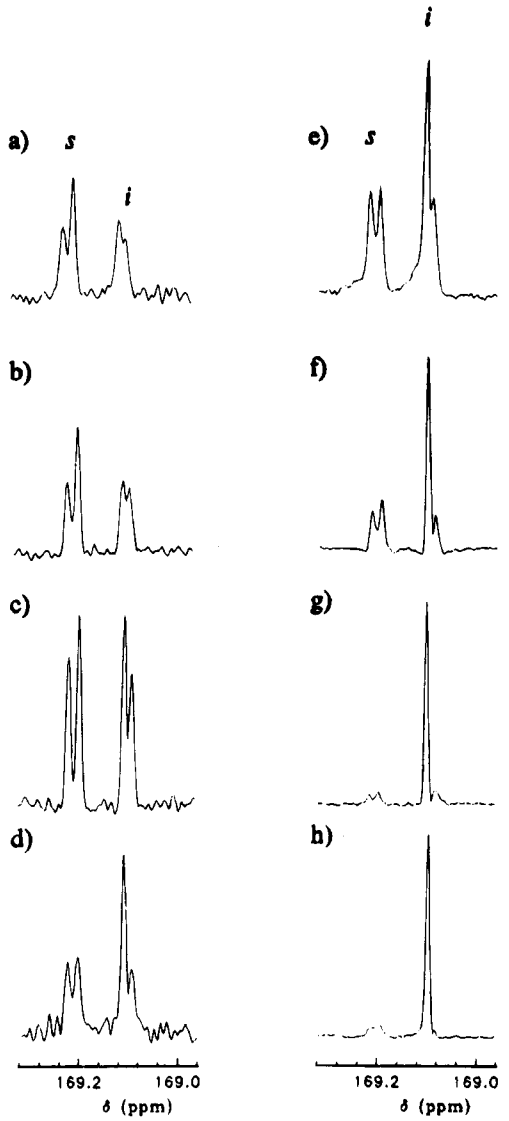

Figure 4. Expansions of the carbonyl resonances for (*R,S*)-PHB in $CDCl_3$ at room temperature: (a) sample with 34% isotactic diads; (b) 40% isotactic diads; (c) 45% isotactic diads; (d) 55% isotactic diads; (e) 60% isotactic diads; (f) 68% isotactic diads; (g) 79% isotactic diads; and (h) 88% isotactic diads.

considered, where the diad intensities were measured by integrating each pair of partly resolved tetrads as a single unit.

Intensities and the Bernoullian Model. The measured peak intensities and adapted Bernoullian triad parameters for each sample, obtained in $CDCl_3$ at room temperature and in TCE-d_2 at 110 °C, are listed in Tables 3 and 4, respectively. The intensities of the *i* diads differ slightly from the percent isotactic diads measured at low resolution; as the high-resolution spectra were obtained under more rigorously quantitative conditions, the new values are likely to more accurately reflect the true sample compositions. For simplicity, the samples will continue to be identified by the percent isotactic diads calculated from the low-resolution spectra. Comparison of the peak intensities obtained in $CDCl_3$ at room temperature and in TCE-d_2 at 110 °C shows that the high-resolution spectra are reasonably consistent with each other, with only minor differences in peak intensities despite the differences in solvent and temperature. The polymerization mechanism is clearly not Bernoullian, as the triad intensities

Table 3. Peak Intensities and Adapted Bernoullian Test Parameters for (*R,S*)-PHB in $CDCl_3$ at Room Temperature

sample (% isotactic diads)	diad intensities[a]		triad intensities[b]				
	i	*s*	*si*	*ii*	*ss*	*is*	B_2[c]
34	0.41	0.59	0.22	0.21	0.37	0.20	1.79
40	0.43	0.57	0.24	0.23	0.36	0.18	1.86
45	0.48	0.52	0.22	0.24	0.29	0.25	1.30
55	0.55	0.45	0.22	0.39	0.21	0.18	2.08
60	0.59	0.41	0.23	0.38	0.20	0.20	1.65
68	0.67	0.33	0.17	0.51	0.16	0.16	3.04
79	0.88	0.12	0.07	0.78	0.07	0.08	10.34
88	0.86	0.14	0.09	0.78	0.06	0.07	7.93

[a] Measured by integrating the components of the carbonyl resonance (~169 ppm). [b] Measured by integrating the components of the methylene resonance (~41 ppm). [c] Calculated using eq 2.

Table 4. Peak Intensities and Adapted Bernoullian Test Parameters for (*R,S*)-PHB in TCE-d_2 at 110 °C

sample (% isotactic diads)	diad intensities[a]		triad intensities[b]				
	i	*s*	*si*	*ii*	*ss*	*is*	B_2[c]
34	0.39	0.61	0.20	0.22	0.39	0.19	2.11
40	0.41	0.59	0.22	0.21	0.37	0.20	1.84
45	0.48	0.52	0.24	0.25	0.28	0.23	1.29
55	0.59	0.41	0.22	0.37	0.22	0.19	1.90
60	0.60	0.40	0.22	0.38	0.20	0.20	1.73
68	0.69	0.31	0.16	0.52	0.16	0.17	3.12
79	0.88	0.12	0.08	0.77	0.08	0.07	10.53
88	0.88	0.12	0.07	0.79	0.07	0.07	11.34

[a] Measured by integrating the components of the carbonyl resonance (~169 ppm). [b] Measured by integrating the components of the methylene resonance (~41 ppm). [c] Calculated using eq 2.

differ dramatically from the predicted Bernoullian intensities of 0.25, 0.25, 0.25, and 0.25.

First-Order Markov Model. The values calculated for B_2 (Tables 3 and 4) for the syndiotactic and low isotactic samples (34–60% isotactic diads) are within the 0.5–2.0 range suggested[58] for compliance with racemic first-order Markov statistics; more isotactic samples are increasingly outside this range. These results for the syndiotactic and low isotactic samples are consistent with those of Kemnitzer et al.,[23] who calculated such values for syndiotactic and atactic (*R,S*)-PHB generated by tin and zinc catalysis, respectively; however, as they did not modify their statistical approach to account for the differences between vinyl chains and chains of PHB, they concluded, based on these results, that the chains followed a Bernoullian model. The fact that test parameters for the more isotactic samples in the current study differ dramatically from the syndiotactic and atactic ones suggests that these more isotactic fractions were formed at a different active site on the aluminoxane catalyst, under conditions where first-order Markov statistics do not apply.

Second-Order Markov Model. To examine the polymerization statistics in more detail, values for $P_{R/SS}$, $P_{R/SR}$, $P_{R/SS} + P_{R/SR}$, Q_2, and $(P_{R/SS} + P_{R/SR})^{-1}$, were calculated for both solvents and temperatures (Tables 5 and 6). Again, results are similar for the different solvents at different temperatures. Examination of the values for $P_{R/SS} + P_{R/SR}$ confirms the trend seen in B_2 above: values are reasonably close to 1.0 for the samples with 34–60% isotactic diads and then decrease progressively with increasing isotacticity. That all values are less than 1.0 indicates that all samples have at least a slight tendency to blockiness, which becomes increasingly pronounced as the samples become more isotactic;

Table 5. Second-Order Markov Parameters for (*R,S*)-PHB in $CDCl_3$ at Room Temperature

sample (% isotactic diads)	$P_{R/SS}$[a]	$P_{R/SR}$[a]	$P_{R/SS} + P_{R/SR}$	ϱ_2[b]	$(P_{R/SS} + P_{R/SR})^{-1}$
34	0.49	0.36	0.86	1.15	1.17
40	0.48	0.37	0.85	1.18	1.17
45	0.49	0.45	0.94	1.07	1.07
55	0.34	0.48	0.82	1.24	1.22
60	0.36	0.52	0.88	1.14	1.14
68	0.24	0.51	0.75	1.36	1.33
79	0.09	0.51	0.59	1.47	1.69
88	0.09	0.56	0.65	1.53	1.54

[a] Calculated using eq 3. [b] Calculated using eq 5.

Table 6. Second-Order Markov Parameters for (*R,S*)-PHB in TCE-d_2 at 110 °C

sample (% isotactic diads)	$P_{R/SS}$[a]	$P_{R/SR}$[a]	$P_{R/SS} + P_{R/SR}$	ϱ_2[b]	$(P_{R/SS} + P_{R/SR})^{-1}$
34	0.48	0.34	0.82	1.20	1.22
40	0.49	0.36	0.85	1.17	1.18
45	0.48	0.46	0.94	1.07	1.07
55	0.36	0.49	0.84	1.18	1.19
60	0.36	0.51	0.87	1.15	1.15
68	0.24	0.51	0.74	1.33	1.34
79	0.09	0.48	0.58	1.42	1.73
88	0.08	0.50	0.58	1.53	1.73

[a] Calculated using eq 3. [b] Calculated using eq 5.

the fact that $P_{R/SS}$ and $P_{R/SR}$ tend to be below 0.5 is a parallel indication of blockiness, while the fact that $P_{R/SS}$ drops well below 0.5 while $P_{R/SR}$ creeps above 0.5 in the more isotactic samples is an indication of an isotactic-like chain (eq 4). The values for ϱ_2 are all above 1.0, also indicating blockiness; the extent to which these values are more than 1.0 increases for the more isotactic samples, again confirming that these are more blocky. The values for ϱ_2 are also close to those for $(P_{R/SS} + P_{R/SR})^{-1}$, showing that these samples fit racemic second-order Markov statistics; the fact that the match is not quite as good for the more isotactic samples could be an indication that these samples do not fit second-order Markov theory quite as well or could just show that the very small intensities of racemic peaks in the highly isotactic spectra are less accurate.

Even without the resolution required to prove or disprove a second-order Markovian mechanism, the fitted conditional probabilities are in keeping with the observed crystallinity behavior. Thus, the blocklike nature of the more isotactic samples observed by NMR corresponds with the strong tendency of these fractions to crystallize with an isotactic crystal structure.[9,12-18] A lesser amount of blockiness in the atactic fractions corresponds with a much reduced crystallinity; although the syndiotactic fractions are less stereoregular than the most isotactic ones, a small increase in blockiness is observed, corresponding with the observed increase in crystallinity.[20,35]

Enantiomorphic Model. As some of the polymer samples are far from adequately described by the first-order Markov model and the validity of the second-order Markov model cannot be proved or disproved with the available data, it is worth considering other models. The observation of blockiness in the samples, particularly the more isotactic ones, suggests that the enantiomorphic model may be suitable, as the combination of *R*- and *S*-preferring sites certainly leads to blockiness.[45,46] Calculated values for the two enantiomorphic test parameters are therefore listed in Table 7. In contrast

Table 7. Test Parameters for the Enantiomorphic Model

sample (% isotactic diads)	in $CDCl_3$ at room temp		in TCE-d_2 at 110 °C	
	E_1[a]	E_2[b]	E_1[a]	E_2[b]
34	1.75	0.26	1.94	0.17
40	1.72	0.26	1.79	0.23
45	1.25	0.62	1.20	0.68
55	1.06	0.86	1.05	0.88
60	0.92	1.22	0.96	1.10
68	0.97	1.11	0.98	1.07
79	0.97	1.18	1.05	0.70
88	0.80	2.81	1.02	0.88

[a] Calculated using eq 9. [b] Calculated using eq 10.

Table 8. Best-Fit Values of the Three Parameters for the Two-Site Model for (*R,S*)-PHB

sample (% isotactic diads)	in $CDCl_3$ at room temp			in TCE-d_2 at 110 °C		
	α	σ_2	ω	α	σ_2	ω
34	0.94	0.36	0.12	0.89	0.33	0.18
40	0.89	0.36	0.17	0.87	0.35	0.17
45	0.80	0.44	0.15	0.80	0.45	0.15
55	0.85	0.48	0.42	0.82	0.48	0.44
60	0.82	0.53	0.37	0.91	0.51	0.24
68	0.95	0.51	0.43	0.87	0.51	0.63
79	0.96	0.51	0.84	0.94	0.46	0.91
88	0.95	0.64	0.84	0.94	0.48	0.94

to the trends in B_2 and $P_{R/SS} + P_{R/SR}$, the values for E_1 and E_2 are closer to 1.0 for the more isotactic samples and farther from 1.0 for the syndiotactic and atactic ones. Thus, although the racemic first-order Markov model reasonably accurately describes the less isotactic samples, the enantiomorphic model better describes the more isotactic ones. This suggests that the two-site model, which involves varying weighting of both racemic first-order Markov and enantiomorphic sites, might describe both tacticity ranges.

Two-Site Model. To obtain values for α, σ, and ω, the three parameters needed to define the two-site model, an iterative technique was used, where the sum of the squares of the differences between measured and calculated triad intensities was minimized. The best fit values for each sample (eqs 11–13) are summarized in Table 8. Despite the lack of longer stereosequences, which would more clearly define exact best-fit values, the reproducibility between the two sets of spectra is reasonably good, implying that the triad data were adequate for the minimization routine employed.

As expected, all values for α are well above 0.5, indicating that the enantiomorphic site yielded primarily isotactic polymer; most of the values for σ_2 are below 0.5, implying that syndiotactic linkages predominate at the first-order Markov site. The values of ω vary systematically, from 0.12–0.17 in the more syndiotactic fractions to 0.84–0.94 in the more isotactic ones, indicating that most of the syndiotactic material was generated at the first-order Markov site, most of the highly isotactic material came from the enantiomorphic site, and the material in the intermediate fractions resulted from a more equal distribution between the two sites. The fact that the isotactic and syndiotactic material could be separated by fractionation indicates that, to a large extent, the material created at each of the two sites was localized in different chains. Some dependence on dynamic equilibria,[43,52] yielding stereoblock chains, could also be occurring; the failure of the two-site model to account for such equilibria could be the source of variation in the values for α and σ_2 between fractions. Alternatively, this variation could

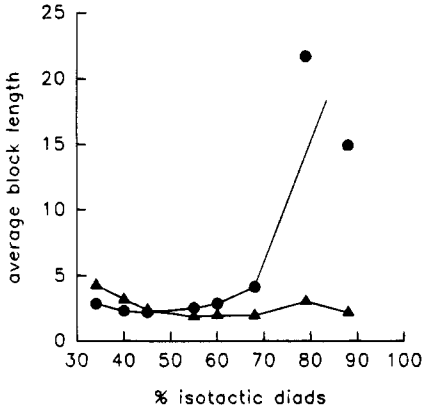

Figure 5. Average block lengths of (*R*,*S*)-PHB: (●) average isotactic block length; (▲) average syndiotactic block length. Calculated using eq 14; averaged over both solvents.

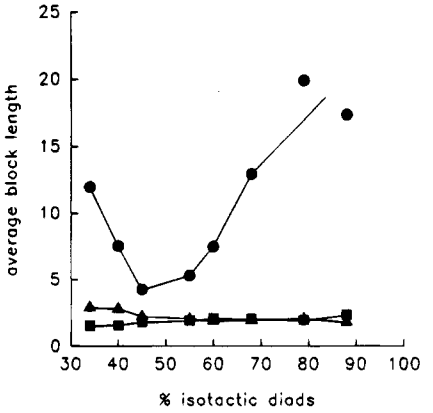

Figure 6. Average block lengths of (*R*,*S*)-PHB at each of the enantiomorphic and first-order Markov sites: (●) isotactic blocks from the enantiomorphic site; (■) isotactic blocks from the first-order Markov site; (▲) syndiotactic blocks from the first-order Markov site. Calculated using eqs 15 and 16; averaged over both solvents.

be a result of small differences in the site characteristics, as the samples were obtained by fractionating the product from several different polymerizations with slight differences in polymerization conditions; another possibility is that more than two sites are involved in the polymerization. Nonetheless, this model appears to be the one which most accurately describes the full range of polymer samples, as characterized by diad and triad intensities.

The agreement of the available stereosequence data with the two-site model can be used to hypothesize on the probable form of blockiness existing in these polymer chains. As the isotactic samples are formed predominantly at the enantiomorphic site, the *R* and *S* sequences tend to be localized in different chains, rather than combined in the same chain, giving structures of the form *RRRRSRRRR* and *SSSSRSSSS* rather than *RRRRSSSS*. As it is difficult to imagine that a predominantly *R* chain and predominantly *S* chain could crystallize together to give exactly the same crystallinity as is present in the all-*R* chains of natural PHB, this implies that the crystallinity in isotactic (*R*,*S*)-PHB involves separate crystals of primarily *R* chains and primarily *S* chains, rather than crystals containing both *R* and *S* isotactic blocks.

Average Block Lengths. For applications such as the interpretation of degradation data or single-crystal results, it is useful to have the samples characterized in terms of the average lengths of isotactic and syndiotactic blocks (Figure 5). As expected, the most isotactic samples, which showed high amounts of blockiness, contain the longest blocks, with an average of 15–22 sequential isotactic diads before a single syndiotactic diad is encountered; the uncertainty in this length is greater than that for shorter block lengths, as observed in other polymers.[59] Despite the strong preference for isotactic diads in these samples, the trend toward blockiness is sufficiently strong that, on average, two or three sequential syndiotactic diads are inserted before the chain begins another isotactic sequence. Thus, the picture of the isotactic chains developed by the two-site model should perhaps be modified from *RRRRSRRRR* and *SSSSRSSSS* to *RRRRSRSRRRR* and *SSSSRSRSSSS*. A similar phenomenon is seen in isotactic polypropylene,[50] where the average racemic block length is two to four even for average isotactic blocks of several hundred. As the (*R*,*S*)-PHB samples become less isotactic, the average isotactic block length steadily decreases while the average syndiotactic block length remains fairly constant until the balance between isotactic and syndiotactic block length shifts toward longer syndiotactic blocks between 45 and 55% isotactic diads. The syndiotactic samples still have sufficient blockiness that, on average, two or three isotactic diads are inserted between syndiotactic sequences.

These data can be used to aid in the interpretation of degradation and single-crystal results. Since enzymatic degradation of these samples using enzymes from *Pseudomonas lemoignei* and *Aspergillus fumigatus* showed that the degradation rate was highest for the samples with 55 and 60% isotactic diads,[34,35] the observation that these samples had an average isotactic block length of four monomer units implies that these enzymes are able to attack *R* sequences of four units or less. As more syndiotactic samples still had average isotactic lengths of three or four monomer units, a small amount of enzymatic degradation could occur in these syndiotactic samples based solely on isotactic content. To examine the formation of isotactic single crystals, the average isotactic block length of 15–22 isotactic diads can be combined with the advance per repeat unit in the crystalline conformation of 3 Å,[18] yielding an average isotactic sequence length of 48–69 Å. This corresponds well with the 50-Å crystalline lamellar thickness for 100% isotactic PHB,[60,61] implying that single crystals of isotactic (*R*,*S*)-PHB[36,37] are composed of crystalline lamellae where the chains within the lamellae are mostly isotactic, with more random sequences in the chain folds.

Assuming that the two-site mechanism gives a reasonable description of the polymer chains, the average block lengths from each of the enantiomorphic and first-order Markovian sites of the catalyst can be calculated.[47,53] For the first-order Markovian site,

$$\bar{n}_{i,\sigma} = 1/(1-\sigma) \qquad \bar{n}_{s,\sigma} = 1/\sigma \tag{15}$$

while at the enantiomorphic site,

$$\bar{n}_{i,\alpha} = \frac{1-2\alpha(1-\alpha)}{\alpha(1-\alpha)} \tag{16}$$

Average syndiotactic block lengths from the enantiomorphic site are considered to be trivial.[53] As shown in Figure 6, material from the first-order Markovian site shows a slight trend toward increasing isotactic block length and decreasing syndiotactic block length with increasing isotacticity. More significantly, the average

isotactic block lengths from the enantiomorphic sites are much greater than those from the first-order Markovian sites; as expected, the isotactic sequences are formed primarily at the enantiomorphic sites. Surprisingly, average isotactic block lengths from the enantiomorphic site are nearly as long in the syndiotactic fractions as in the strongly isotactic ones; as the values of ω for the syndiotactic samples are low, the number of such sequences in the syndiotactic samples is small.

Conclusions

High-resolution ^{13}C NMR spectra for racemic PHB of a wide range of tacticities were obtained both in $CDCl_3$ at room temperature and in TCE-d_2 at 110 °C. Some tetrad splitting was observed, particularly in the $CDCl_3$, but only diads and triads could be completely resolved, limiting the statistical interpretation to that which involves only these peak intensities. Because of the structure of the (*R,S*)-PHB chain, the conventional statistics used for vinyl polymers required adaptation; by the statistical measure appropriate for this polymer, none of the isolated fractions obeyed Bernoullian statistics. Various tests for racemic first-order Markov statistics showed that the syndiotactic and low isotactic samples follow these statistics reasonably well, while highly isotactic samples did not; this suggests that the catalyst contains at least two active sites, with syndiotactic and low isotactic samples forming at a site where the mechanism is independent of the stereoconfiguration of the growing chain end and highly isotactic chains forming at a different site with a tendency to form isotactic blocks. Calculation of the conditional probabilities of racemic second-order Markov statistics confirmed the blocky nature of the more isotactic samples, but this model could not be tested without access to longer stereosequences.

A one-parameter enantiomorphic model showed a better match for the isotactic samples but a poorer one for the syndiotactic ones; it is therefore proposed that a two-site model involving both first-order Markovian and enantiomorphic sites, similar to that used to describe stereospecific polypropylene, be considered. Best-fit values obtained for the three parameters which describe this model match well with predicted trends; more rigorous testing of this model requires longer stereosequences than are currently available. Calculation of average isotactic and syndiotactic block lengths indicates that, even in the most isotactic samples, there are syndiotactic sequences of more than one isolated unit. Use of these block lengths aids in the interpretation of degradation and single-crystal results. If the two-site model is taken as representative of the polymer structures, the syndiotactic fractions could contain a small proportion of long isotactic sequences, derived from the enantiomorphic sites.

Acknowledgment. This work was supported by Xerox Corp. and by a fellowship grant to P.J.H. by the Natural Sciences and Engineering Research Council of Canada.

References and Notes

(1) Holmes, P. A. In *Developments in Crystalline Polymers*; Basset, D. C., Ed.; Elsevier: New York, 1989; Vol. 2, Chapter 1.
(2) Anderson, A. J.; Dawes, E. A. *Microbiol. Rev.* **1990**, *54*, 450–472.
(3) Doi, Y. *Microbial Polyesters*; VCH: New York, 1990.
(4) Steinbüchel, A. In *Biomaterials*; Byrom, D., Ed.; MacMillan: London, 1991; Chapter 3.
(5) Inoue, Y.; Yoshie, N. *Prog. Polym. Sci.* **1992**, *17*, 571–610.
(6) Hocking, P. J.; Marchessault, R. H. In *Chemistry and Technology of Biodegradable Polymers*; Griffin, G. J. L., Ed.; Blackie A & P: Glasgow, U.K., 1994; Chapter 4.
(7) Poirier, Y.; Dennis, D.; Klomparens, K.; Nawrath, C.; Somerville, C. *FEMS Microbiol. Rev.* **1992**, *103*, 237–246.
(8) Poirier, Y.; Dennis, D. E.; Klomparens, K.; Somerville, C. *Science* **1992**, *256*, 520–523.
(9) Zhang, Y.; Gross, R. A.; Lenz, R. W. *Macromolecules* **1990**, *23*, 3206–3212.
(10) Takeichi, T.; Hieda, Y.; Takayama, Y. *Polym. J.* **1988**, *20*, 159–162.
(11) Le Borgne, A.; Spassky, N. *Polymer* **1989**, *30*, 2312–2319.
(12) Agostini, D. E.; Lando, J. B.; Shelton, J. R. *J. Polym. Sci., Polym. Chem. Ed.* **1971**, *9*, 2775–2787.
(13) Tani, H.; Yamashita, S.; Teranishi, K. *Polym. J.* **1972**, *3*, 417–418.
(14) Teranishi, K.; Iida, M.; Araki, T.; Yamashita, S.; Tani, H. *Macromolecules* **1974**, *7*, 421–427.
(15) Iida, M.; Araki, T.; Teranishi, K.; Tani, H. *Macromolecules* **1977**, *10*, 275–284.
(16) Bloembergen, S.; Holden, D. A.; Bluhm, T. L.; Hamer, G. K.; Marchessault, R. H. *Macromolecules* **1989**, *22*, 1656–1663.
(17) Benvenuti, M.; Lenz, R. W. *J. Polym. Sci., Polym. Chem. Ed.* **1991**, *29*, 793–805.
(18) Yokouchi, M.; Chatani, Y.; Tadokoro, H.; Teranishi, K.; Tani, H. *Polymer* **1973**, *14*, 267–272.
(19) Bloembergen, S.; Holden, D. A.; Bluhm, T. L.; Hamer, G. K.; Marchessault, R. H. *Macromolecules* **1989**, *22*, 1663–1669.
(20) Hocking, P. J.; Marchessault, R. H. *Polym. Bull.* **1993**, *30*, 163–170.
(21) Kemnitzer, J. E.; McCarthy, S. P.; Gross, R. A. *Macromolecules* **1993**, *26*, 1221–1229.
(22) Hori, Y.; Suzuki, M.; Yamaguchi, A.; Nishishita, T. *Macromolecules* **1993**, *26*, 5533–5534.
(23) Kemnitzer, J. E.; McCarthy, S. P.; Gross, R. A. *Macromolecules* **1993**, *26*, 6143–6150.
(24) Abe, H.; Matsubara, I.; Doi, Y.; Hori, Y.; Yamaguchi, A. *Macromolecules* **1994**, *27*, 6018–6025.
(25) Kricheldorf, H. R.; Lee, S.-R.; Scharnagl, N. *Macromolecules* **1994**, *27*, 3139–3146.
(26) Doi, Y.; Kunoika, M.; Nakamura, Y.; Soga, K. *Macromolecules* **1986**, *19*, 2860–2864.
(27) Bluhm, T. L.; Hamer, G. K.; Marchessault, R. H.; Fyfe, C. A.; Veregin, R. P. *Macromolecules* **1986**, *19*, 2871–2876.
(28) Kamiya, N.; Yamamoto, Y.; Inoue, Y.; Chûjô, R.; Doi, Y. *Macromolecules* **1989**, *22*, 1676–1682.
(29) Inoue, Y.; Kamiya, N.; Yamamoto, Y.; Chûjô, R.; Doi, Y. *Macromolecules* **1989**, *22*, 3800–3802.
(30) Bloembergen, S.; Holden, D. A.; Bluhm, T. L.; Hamer, G. K.; Marchessault, R. H. *Macromolecules* **1987**, *20*, 3086–3089.
(31) Doi, Y.; Kumagai, Y.; Tanahashi, N.; Mukai, K. In *Biodegradable Polymers and Plastics*; Vert, M., Feijen, J., Albertsson, A., Scott, G., Chiellini, E., Eds.; Special Publication No. 109; Royal Society of Chemistry: Cambridge, U.K., 1992; pp 139–147.
(32) Kemnitzer, J. E.; McCarthy, S. P.; Gross, R. A. *Macromolecules* **1992**, *25*, 5927–5934.
(33) Jesudason, J. J.; Marchessault, R. H.; Saito, T. *J. Environ. Polym. Degrad.* **1993**, *1*, 89–98.
(34) Hocking, P. J.; Marchessault, R. H.; Timmins, M. R.; Scherer, T. M.; Lenz, R. W.; Fuller, R. C. *Makromol. Rapid Commun.* **1994**, *15*, 447–452.
(35) Hocking, P. J.; Timmins, M. R.; Scherer, T. M.; Fuller, R. C.; Lenz, R. W.; Marchessault, R. H. *J. Macromol. Sci., Chem.* **1995**, *A32*, 889–994.
(36) Orts, W. J. Ph.D. Thesis, University of Toronto, Toronto, Ontario, Canada, 1991.
(37) Hocking, P. J.; Marchessault, R. H., in preparation.
(38) Bovey, F. A.; Jelinski, L. W. *Chain Structure and Conformation of Macromolecules*; Academic: New York, 1982; Chapter 3.
(39) Bovey, F. A. *High Resolution NMR of Macromolecules*; Academic: New York, 1972; Chapter 8.
(40) Bovey, F. A. *Polymer Conformation and Configuration*; Academic: New York, 1969; Chapters 1 and 2.
(41) Hiemenz, P. C. *Polymer Chemistry, The Basic Concepts*; Marcel Dekker: New York, 1984; pp 471–488.
(42) Sepulchre, M. *Makromol. Chem.* **1988**, *189*, 1117–1131.
(43) Coleman, B. D.; Fox, T. G. *J. Chem. Phys.* **1963**, *38*, 1065–1075.
(44) Coleman, B. D.; Fox, T. G. *J. Polym. Sci., Part A* **1963**, *1*, 3183–3197.

(45) Schuerch, C. *J. Polym. Sci.* **1959**, *40*, 533–536.
(46) Sheldon, R. A.; Fueno, T.; Tsunetsugu, T.; Furukawa, J. *J. Polym. Sci., Polym. Lett. Ed.* **1965**, *3*, 23–26.
(47) Inoue, Y.; Itabashi, Y.; Chûjô, R.; Doi, Y. *Polymer* **1984**, *25*, 1640–1644.
(48) Doi, Y. *Makromol. Chem., Rapid Commun.* **1982**, *3*, 635–641.
(49) Zhu, S. N.; Yang, X. Z.; Chûjô, R. *Polym. J.* **1983**, *15*, 859–868.
(50) Paukkeri, R.; Väänänen, T.; Lehtinen, A. *Polymer* **1993**, *34*, 2488–2494.
(51) Chûjô, R.; Kogure, Y.; Väänänen, T. *Polymer* **1994**, *35*, 339–342.
(52) Coleman, B. D.; Fox, T. G. *J. Am. Chem. Soc.* **1963**, *85*, 1241–1244.
(53) Chûjô, R. *J. Macromol. Sci., Phys.* **1968**, *B2*, 1–11.
(54) Bovey, F. A. *High Resolution NMR of Macromolecules*; Academic: New York, 1972; Chapter 1.
(55) Koenig, J. L. *Spectroscopy of Polymers*; American Chemical Society: Washington, DC, 1992; Chapters 1 and 6.
(56) Primrose, W. U. In *NMR of Macromolecules, A Practical Approach*; Roberts, G. C. K., Ed.; Oxford University Press: New York, 1993; Chapter 2.
(57) Metanomski, W. V. *Compendium of Macromolecular Nomenclature*; Blackwell Scientific: Boston, 1991; pp 91–109.
(58) Pino, P.; Suter, U. W. *Polymer* **1976**, *17*, 977–995; *Polymer* **1977**, *18*, 412.
(59) Randall, J. C. *J. Polym. Sci., Polym. Phys. Ed.* **1976**, *14*, 2083–2094.
(60) Marchessault, R. H.; Coulombe, S.; Morikawa, H.; Okamura, K.; Revol, J. F. *Can. J. Chem.* **1981**, *59*, 38–44.
(61) Revol, J. F.; Chanzy, H. D.; Deslandes, Y.; Marchessault, R. H. *Polymer* **1989**, *30*, 1973–1976.

MA9503874